SUPPLEMENTAL MATERIAL FOR

Order and disorder in quaternary atomic laminates from first-principles calculations

Martin Dahlqvist and Johanna Rosen

Thin Film Physics Division, Department of Physics, Chemistry and Biology (IFM), Linköping University, SE-581 83 Linköping, Sweden

Additional material for considered spin configurations used to model Cr-based MAX phases

Detailed information for considered magnetic spin configurations used to model antiferromagnetic Cr-based MAX phases are given in Table S1 to S4 for TiCrAlC, Table S5 and S6 for $CrTi_2AlC_2$, Table S7 and S8 for $TiCr_2AlC_2$, and Table S9 and S10 for $Ti_2Cr_2AlC_3$.

Table S1 Primitive translation vectors P_i and atomic coordinates for the *M*-sites in a 1×1×1 M_2AX unit cell used to calculate AFM1 spin configurations for different ordered layered TiCrAlC phases, the type given within parenthesis. Spin up and spin down for individual Cr atoms are indicated by (+) and (–), respectively.

Type	*x*	*y*	*z*	Spin configuration		
				AFM1 (A)	AFM1 (B)	AFM1 (C)
P_1	$a/2$	$-a\sqrt{3}/2$	0			
P_2	$a/2$	$a\sqrt{3}/2$	0			
P_3	0	0	c			
M	$a/2$	$a/(2\sqrt{3})$	zc	+	+	+
M	$a/2$	$a/(2\sqrt{3})$	$(1/2-z)c$			–
M	$a/2$	$-a/(2\sqrt{3})$	$(1/2+z)c$		–	
M	$a/2$	$-a/(2\sqrt{3})$	$-zc$	–		

Table S2 Primitive translation vectors P_i and atomic coordinates for the *M*-sites in a 2×1×1 M_2AX unit cell used to calculate in-AFM1 and in-AFM2 spin configurations for different ordered layered TiCrAlC phases, type given within parenthesis. Spin up and spin down for individual Cr atoms are indicated by (+) and (–), respectively.

Type	*x*	*y*	*z*	Spin configuration					
				in-AFM1 (A)	in-AFM2 (A)	in-AFM1 (B)	in-AFM2 (B)	in-AFM1 (C)	in-AFM2 (C)
P_1	a	$-a\sqrt{3}$	0						
P_2	$a/2$	$a\sqrt{3}/2$	0						
P_3	0	0	c						
M	$a/2$	$a/(2\sqrt{3})$	zc	–	+	+	+	+	+
M	*a*	$-a/\sqrt{3}$	zc	+	–	–	–	–	–
M	$a/2$	$a/(2\sqrt{3})$	$(1/2-z)c$					–	+
M	*a*	$-a/\sqrt{3}$	$(1/2-z)c$					+	–
M	$a/2$	$-a/(2\sqrt{3})$	$(1/2+z)c$			–	+		
M	*a*	$-2a/\sqrt{3}$	$(1/2+z)c$			+	–		
M	$a/2$	$-a/(2\sqrt{3})$	$-zc$	+	+				
M	*a*	$-2a/\sqrt{3}$	$-zc$	–	–				

Table S3 Primitive translation vectors P_i and atomic coordinates for the *M*-sites in a 1×1×2 M_2AX unit cell used to calculate AFM1 spin configurations for type D ordered layered TiCrAlC phases. Spin up and spin down for individual Cr atoms are indicated by (+) and (–), respectively.

Type	*x*	*y*	*z*	Spin configuration		
				AFM1 (D)	AFM2 (D)	AFM3 (D)
P_1	$a/2$	$-a\sqrt{3}/2$	0			
P_2	$a/2$	$a\sqrt{3}/2$	0			
P_3	0	0	$2c$			
M	$a/2$	$a/(2\sqrt{3})$	zc	+	+	–
M	$a/2$	$a/(2\sqrt{3})$	$(1/2-z)c$			
M	$a/2$	$-a/(2\sqrt{3})$	$(1/2+z)c$			
M	$a/2$	$-a/(2\sqrt{3})$	$-zc$			
M	$a/2$	$a/(2\sqrt{3})$	$(1+z)c$			
M	$a/2$	$a/(2\sqrt{3})$	$(3/2-z)c$	–	+	+
M	$a/2$	$-a/(2\sqrt{3})$	$(3/2+z)c$	–	–	–
M	$a/2$	$-a/(2\sqrt{3})$	$(1-z)c$	+	–	+

Table S4 Primitive translation vectors P_i and atomic coordinates for the *M*-sites in a 2×1×1 M_2AX unit cell used to calculate in-AFM1 and in-AFM2 spin configurations for type D ordered layered TiCrAlC phases. Spin up and spin down for individual Cr atoms are indicated by (+) and (–), respectively.

Type	*x*	*y*	*z*	Spin configuration	
				in-AFM1 (D)	in-AFM2 (D)
P_1	a	$-a\sqrt{3}$	0		
P_2	$a/2$	$a\sqrt{3}/2$	0		
P_3	0	0	$2c$		
M	$a/2$	$a/(2\sqrt{3})$	zc	+	+
M	*a*	$-a/\sqrt{3}$	zc	–	–
M	$a/2$	$a/(2\sqrt{3})$	$(1/2-z)c$		
M	*a*	$-a/\sqrt{3}$	$(1/2-z)c$		
M	$a/2$	$-a/(2\sqrt{3})$	$(1/2+z)c$		
M	*a*	$-2a/\sqrt{3}$	$(1/2+z)c$		
M	$a/2$	$-a/(2\sqrt{3})$	$-zc$		
M	*a*	$-2a/\sqrt{3}$	$-zc$		
M	$a/2$	$a/(2\sqrt{3})$	$(1+z)c$		
M	*a*	$-a/\sqrt{3}$	$(1+z)c$		
M	$a/2$	$a/(2\sqrt{3})$	$(3/2-z)c$	–	+
M	*a*	$-a/\sqrt{3}$	$(3/2-z)c$	+	–
M	$a/2$	$-a/(2\sqrt{3})$	$(3/2+z)c$	–	+
M	*a*	$-2a/\sqrt{3}$	$(3/2+z)c$	+	–
M	$a/2$	$-a/(2\sqrt{3})$	$(1-z)c$	+	+
M	*a*	$-2a/\sqrt{3}$	$(1-z)c$	–	–

Table S5 Primitive translation vectors P_i and atomic coordinates for the M-sites in a 1×1×1 M_3AX_2 unit cell used to calculate AFM1 spin configurations for different ordered layered $CrTi_2AlC$ phases, type given within parenthesis. Spin up and spin down for individual Cr atoms are indicated by (+) and (–), respectively.

Type	x	y	z	Spin configuration					
				AFM1 (A)	AFM1 (B)	AFM1 (C)	AFM1 (D)	AFM1 (E)	AFM1 (F)
P_1	$a/2$	$-a\sqrt{3}/2$	0						
P_2	$a/2$	$a\sqrt{3}/2$	0						
P_3	0	0	c						
M	$a/2$	$a/(2\sqrt{3})$	$-zc$		+	+		+	+
M	0	0	0	+				–	
M	$a/2$	$-a/(2\sqrt{3})$	zc				+		–
M	$a/2$	$-a/(2\sqrt{3})$	$(1/2-z)c$			–	–		
M	0	0	$c/2$	–	–				
M	$a/2$	$a/(2\sqrt{3})$	$(1/2+z)c$						

Table S6 Primitive translation vectors P_i and atomic coordinates for the *M*-sites in a 2×1×1 M_3AX_2 unit cell used to calculate in-AFM1 and in-AFM2 spin configurations for ordered layered $CrTi_2AlC_3$ phases, type given within parenthesis. Spin up and spin down for individual Cr atoms are indicated by (+) and (–), respectively

Type	*x*	*y*	*z*	Spin configuration					
				in-AFM1 (A)	in-AFM2 (A)	in-AFM1 (B)	in-AFM2 (B)	in-AFM1 (C)	in-AFM2 (C)
P_1	a	$-a\sqrt{3}$	0						
P_2	$a/2$	$a\sqrt{3}/2$	0						
P_3	0	0	c						
M	$a/2$	$a/(2\sqrt{3})$	$-zc$			+	+	+	+
M	*a*	$-a/\sqrt{3}$	$-zc$			–	–	–	–
M	0	0	0	+	+				
M	$a/2$	$-a/\sqrt{2}$	0	–	–				
M	$a/2$	$-a/(2\sqrt{3})$	zc						
M	*a*	$-2a/\sqrt{3}$	zc						
M	$a/2$	$-a/(2\sqrt{3})$	$(1/2-z)c$					–	+
M	*a*	$-2a/\sqrt{3}$	$(1/2-z)c$					+	–
M	0	0	$c/2$	–	+	–	+		
M	$a/2$	$-a/\sqrt{2}$	$c/2$	+	–	+	–		
M	$a/2$	$a/(2\sqrt{3})$	$(1/2+z)c$						
M	*a*	$-a/\sqrt{3}$	$(1/2+z)c$						
				in-AFM1 (D)	in-AFM2 (D)	in-AFM1 (E)	in-AFM2 (E)	in-AFM1 (F)	in-AFM2 (F)
M	$a/2$	$a/(2\sqrt{3})$	$-zc$						
M	*a*	$-a/\sqrt{3}$	$-zc$						
M	0	0	0						
M	$a/2$	$-a/\sqrt{2}$	0						
M	$a/2$	$-a/(2\sqrt{3})$	zc	+	+				
M	*a*	$-2a/\sqrt{3}$	zc	–	–				
M	$a/2$	$-a/(2\sqrt{3})$	$(1/2-z)c$	–	+	+	+	+	+
M	*a*	$-2a/\sqrt{3}$	$(1/2-z)c$	+	–	–	–	–	–
M	0	0	$c/2$			–	+		
M	$a/2$	$-a/\sqrt{2}$	$c/2$			+	–		
M	$a/2$	$a/(2\sqrt{3})$	$(1/2+z)c$					–	+
M	*a*	$-a/\sqrt{3}$	$(1/2+z)c$					+	–

Table S7 Primitive translation vectors P_i and atomic coordinates for the *M*-sites in a 1×1×1 M_3AX_2 unit cell used to calculate different AFM spin configurations for different ordered layered $TiCr_2AlC$ phases, type given within parenthesis. Spin up and spin down for individual Cr atoms are indicated by (+) and (–), respectively.

Type	*x*	*y*	*z*	Spin configuration								
				AFM1 (A)	AFM2 (A)	AFM3 (A)	AFM1 (B)	AFM2 (B)	AFM3 (B)	AFM1 (C)	AFM2 (C)	AFM3 (C)
P_1	$a/2$	$-a\sqrt{3}/2$	0									
P_2	$a/2$	$a\sqrt{3}/2$	0									
P_3	0	0	c									
M	$a/2$	$a/(2\sqrt{3})$	$-zc$	+	–	+						
M	0	0	0				+	–	+	+	–	+
M	$a/2$	$-a/(2\sqrt{3})$	zc	+	+	–	+	+	–	+	+	–
M	$a/2$	$-a/(2\sqrt{3})$	$(1/2-z)c$	–	+	+	–	+	+			
M	0	0	$zc/2$							–	+	+
M	$a/2$	$a/(2\sqrt{3})$	$(1/2+z)c$	–	–	–	–	–	–	–	–	–
				AFM1 (D)	AFM2 (D)	AFM3 (D)	AFM1 (E)	AFM2 (E)	AFM3 (E)	AFM1 (F)	AFM2 (F)	AFM3 (F)
M	$a/2$	$a/(2\sqrt{3})$	$-zc$	+	–	+	+	+	+	+	+	+
M	0	0	0	+	+	–	+	+	–	+	+	–
M	$a/2$	$-a/(2\sqrt{3})$	zc				+	–	+	+	–	+
M	$a/2$	$-a/(2\sqrt{3})$	$(1/2-z)c$				–	–	–			
M	0	0	$zc/2$	–	+	+				–	–	–
M	$a/2$	$a/(2\sqrt{3})$	$(1/2+z)c$	–	–	–						

Table S8 Primitive translation vectors P_i and atomic coordinates for the *M*-sites in a 2×1×1 M_3AX_2 unit cell used to calculate in-AFM1 and in-AFM2 spin configurations for ordered layered $TiCr_2AlC_3$ phases, type given within parenthesis. Spin up and spin down for individual Cr atoms are indicated by (+) and (–), respectively

Type	*x*	*y*	*z*	Spin configuration					
				in-AFM1 (A)	in-AFM2 (A)	in-AFM1 (B)	in-AFM2 (B)	in-AFM1 (C)	in-AFM2 (C)
P_1	a	$-a\sqrt{3}$	0						
P_2	$a/2$	$a\sqrt{3}/2$	0						
P_3	0	0	c						
M	$a/2$	$a/(2\sqrt{3})$	$-zc$	+	+				
M	*a*	$-a/\sqrt{3}$	$-zc$	–	–				
M	0	0	0			+	+	+	+
M	$a/2$	$-a/\sqrt{2}$	0			–	–	–	–
M	$a/2$	$-a/(2\sqrt{3})$	zc	–	+	–	+	–	+
M	*a*	$-2a/\sqrt{3}$	zc	+	–	+	–	+	–
M	$a/2$	$-a/(2\sqrt{3})$	$(1/2-z)c$	–	+	–	+		
M	*a*	$-2a/\sqrt{3}$	$(1/2-z)c$	+	–	+	–		
M	0	0	$zc/2$					–	+
M	$a/2$	$-a/\sqrt{2}$	$zc/2$					+	–
M	$a/2$	$a/(2\sqrt{3})$	$(1/2+z)c$	+	+	+	+	+	+
M	*a*	$-a/\sqrt{3}$	$(1/2+z)c$	–	–	–	–	–	–
				in-AFM1 (D)	in-AFM2 (D)	in-AFM1 (E)	in-AFM2 (E)	in-AFM1 (F)	in-AFM2 (F)
M	$a/2$	$a/(2\sqrt{3})$	$-zc$	+	+	+	+	+	+
M	*a*	$-a/\sqrt{3}$	$-zc$	–	–	–	–	–	–
M	0	0	0	–	+	–	+	–	+
M	$a/2$	$-a/\sqrt{2}$	0	+	–	+	–	+	–
M	$a/2$	$-a/(2\sqrt{3})$	zc			+	+	+	+
M	*a*	$-2a/\sqrt{3}$	zc			–	–	–	–
M	$a/2$	$-a/(2\sqrt{3})$	$(1/2-z)c$						
M	*a*	$-2a/\sqrt{3}$	$(1/2-z)c$						
M	0	0	$zc/2$	–	+			–	+
M	$a/2$	$-a/\sqrt{2}$	$zc/2$	+	–			+	–
M	$a/2$	$a/(2\sqrt{3})$	$(1/2+z)c$	+	+	–	+		
M	*a*	$-a/\sqrt{3}$	$(1/2+z)c$	–	–	+	–		

Table S9 Primitive translation vectors P_i and atomic coordinates for the *M*-sites in a 1×1×1 M_4AX_3 unit cell used to calculate different AFM spin configurations for ordered layered $Ti_2Cr_2AlC_3$ (A) and $Cr_2Ti_2AlC_3$ (B) phases, type given within parenthesis. Spin up and spin down for individual Cr atoms are indicated by (+) and (–), respectively.

Type	*x*	*y*	*z*	Spin configuration					
				AFM1 (A)	AFM2 (A)	AFM3 (A)	AFM1 (B)	AFM2 (B)	AFM3 (B)
P_1	$a/2$	$-a\sqrt{3}/2$	0						
P_2	$a/2$	$a\sqrt{3}/2$	0						
P_3	0	0	c						
M	0	0	$-z_2c$	+	–	+			
M	$a/2$	$a/(2\sqrt{3})$	$-z_1c$				+	+	+
M	$a/2$	$-a/(2\sqrt{3})$	z_1c				+	–	–
M	0	0	z_2c	+	+	–			
M	0	0	$(1/2-z_2)c$	–	+	+			
M	$a/2$	$-a/(2\sqrt{3})$	$(1/2-z_1)c$				–	–	+
M	$a/2$	$a/(2\sqrt{3})$	$(1/2+z_1)c$				–	+	–
M	0	0	$(1/2+z_2)c$	–	–	–			

Table S10 Primitive translation vectors P_i and atomic coordinates for the *M*-sites in a 2×1×1 M_4AX_3 unit cell used to calculate in-AFM1 and in-AFM2 spin configurations for ordered layered $Ti_2Cr_2AlC_3$ (A) and $Cr_2Ti_2AlC_3$ (B) phases, type given within parenthesis. Spin up and spin down for individual Cr atoms are indicated by (+) and (–), respectively

Type	*x*	*y*	*z*	Spin configuration			
				in-AFM1 (A)	in-AFM2 (A)	in-AFM1 (B)	in-AFM2 (B)
P_1	a	$-a\sqrt{3}$	0				
P_2	$a/2$	$a\sqrt{3}/2$	0				
P_3	0	0	c				
M	0	0	$-z_2c$	+	+		
M	$a/2$	$-a/\sqrt{2}$	$-z_2c$	–	–		
M	$a/2$	$a/(2\sqrt{3})$	$-z_1c$			+	+
M	a	$-a/\sqrt{3}$	$-z_1c$			–	–
M	$a/2$	$-a/(2\sqrt{3})$	z_1c			–	+
M	a	$-2a/\sqrt{3}$	z_1c			+	–
M	0	0	z_2c	+	+		
M	$a/2$	$-a/\sqrt{2}$	z_2c	–	–		
M	0	0	$(1/2-z_2)c$	–	+		
M	$a/2$	$-a/\sqrt{2}$	$(1/2-z_2)c$	+	–		
M	$a/2$	$-a/(2\sqrt{3})$	$(1/2-z_1)c$			+	+
M	a	$-2a/\sqrt{3}$	$(1/2-z_1)c$			–	–
M	$a/2$	$a/(2\sqrt{3})$	$(1/2+z_1)c$			–	+
M	a	$-a/\sqrt{3}$	$(1/2+z_1)c$			+	–
M	0	0	$(1/2+z_2)c$	–	+		
M	$a/2$	$-a/\sqrt{2}$	$(1/2+z_2)c$	+	–		

Additional material for considered atomic stackings for MC and $M_{n+1}AC_n$ phases

Figure S1 schematically illustrates the atomic stacking for six different MC type structures. Fig. S2 to S4 show schematic illustrations of different atomic stacking for M_2AX, M_3AX_2, and M_4AX_3 composition. Fig. S5 show formation enthalpy ΔH_{cp} as function of volume for all considered atomic stacking sequences of $M_{n+1}AlC_n$ (n = 1 – 3). Fig. S6 displays formation enthalpy ΔH_{cp} as function of volume for all considered atomic stacking sequences for ordered layers of type A of MTi$_2$AlC$_2$ and TiM_2AlC$_2$ whereas Fig. S7 show formation enthalpy ΔH_{cp} as function of volume for all considered atomic stacking sequences for Ti$_2M_2$AlC$_3$ of type A and B.

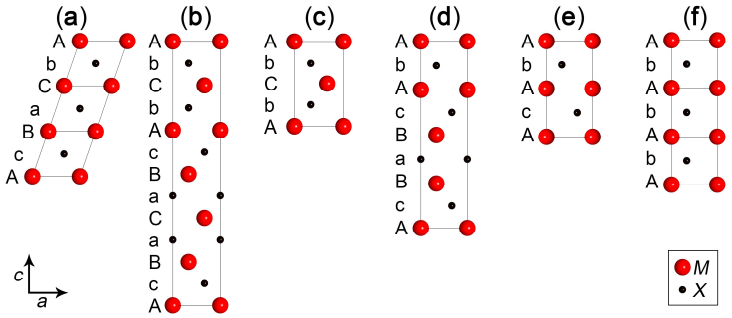

Fig. S1 Schematic illustration of different stackings of MX composition for type structures (a) NaCl, (b) η-MoC, (c) NiAs, (d) γ'-MoC, (e) δ-NbN, (f) and (f) WC. For visual comparison the 111 plane of cubic NaCl is perpendicular to the c-axis of the other type structures.

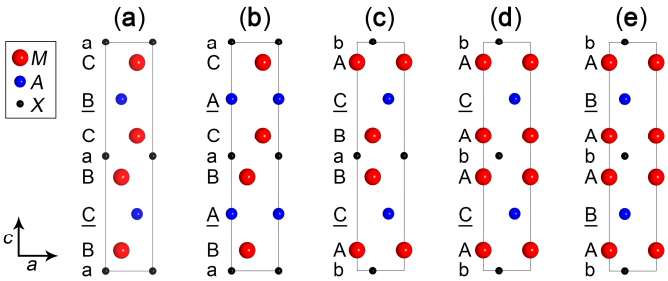

Fig. S2 Schematic illustration of five different stackings of M_2AX composition where (a) represents the archetypical Cr$_2$AlC MAX phase structure and (b) β-Ti$_2$AlC.

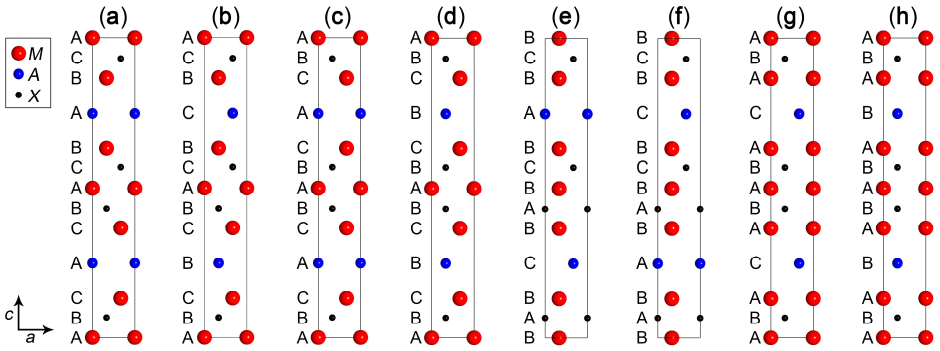

Fig. S3 Schematic illustration of seven different stackings of M_3AX_2 composition where (a) represents the archetypical α-Ti_3SiC_2 MAX phase structure and (b) β-Ti_3SiC_2.

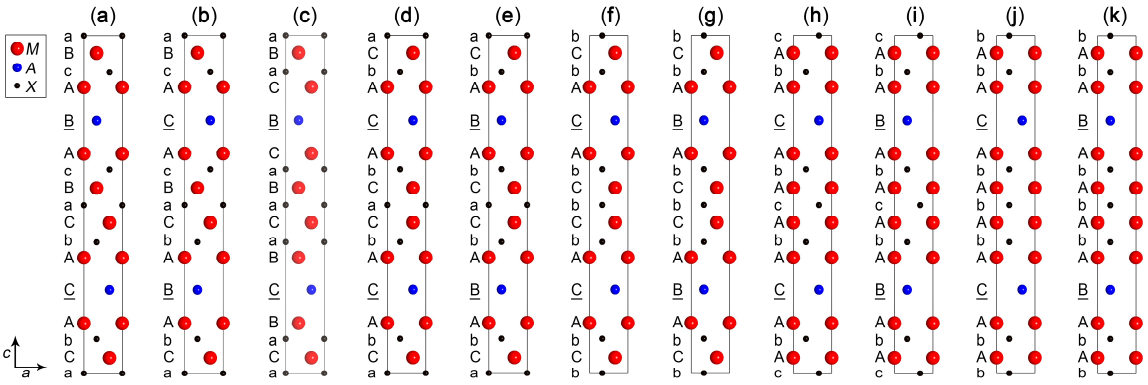

Fig. S4 Schematic illustration of nine different stackings of M_4AX_3 composition where (a) represents the archetypical Ti_4AlN_3 MAX phase structure, (b) γ-Ti_4GaC_3, and (c) β-Ta_4AlC_3.

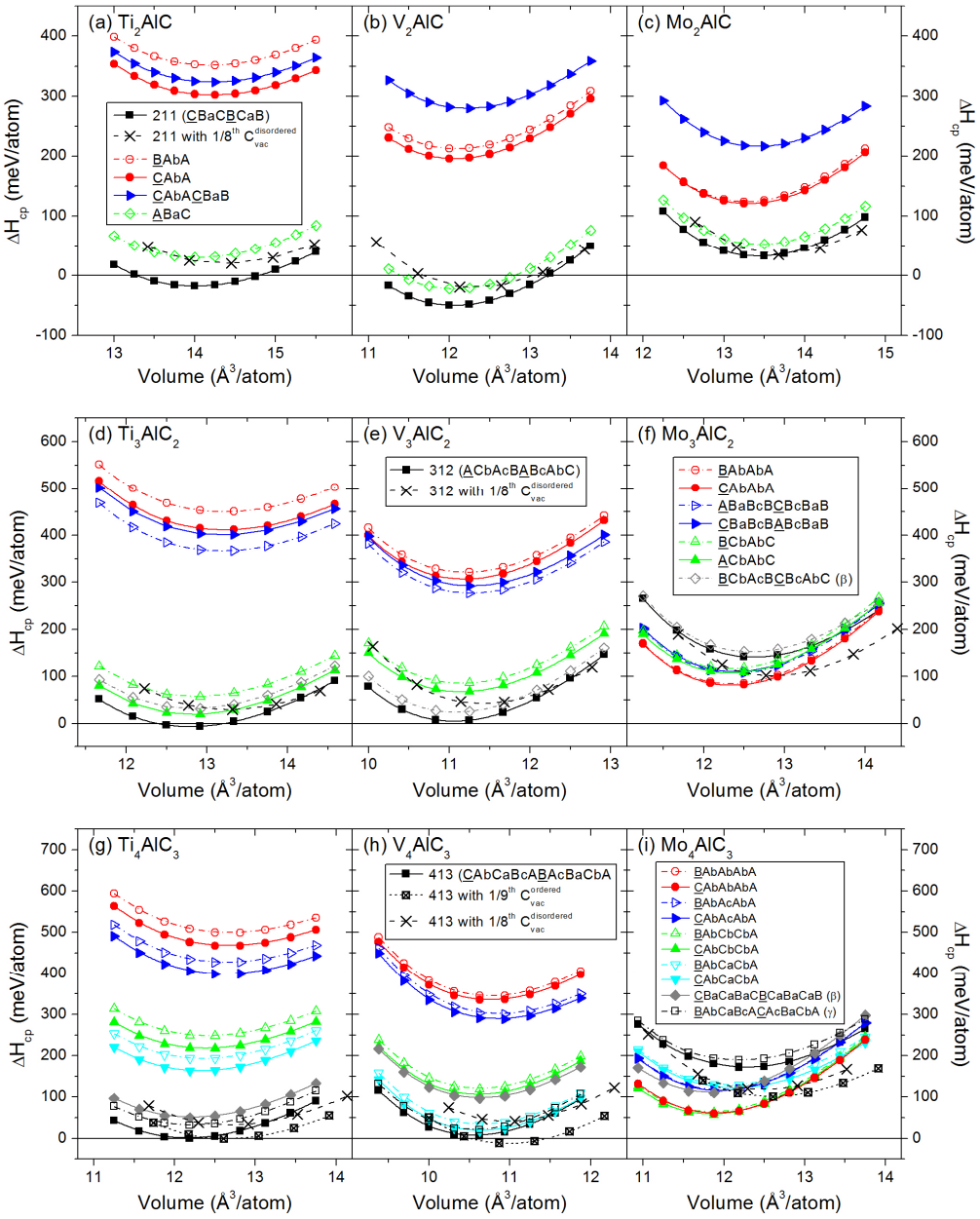

Fig. S5 Formation enthalpy ΔH_{cp} for different atomic stacking sequences of $M_{n+1}AlC_n$ ($n = 1 - 3$) where M = Ti, V, and Mo. For the MAX phase stacking (black symbols), disordered and ordered carbon vacancies have also been modelled for $n = 1 - 3$ and $n = 3$, respectively.

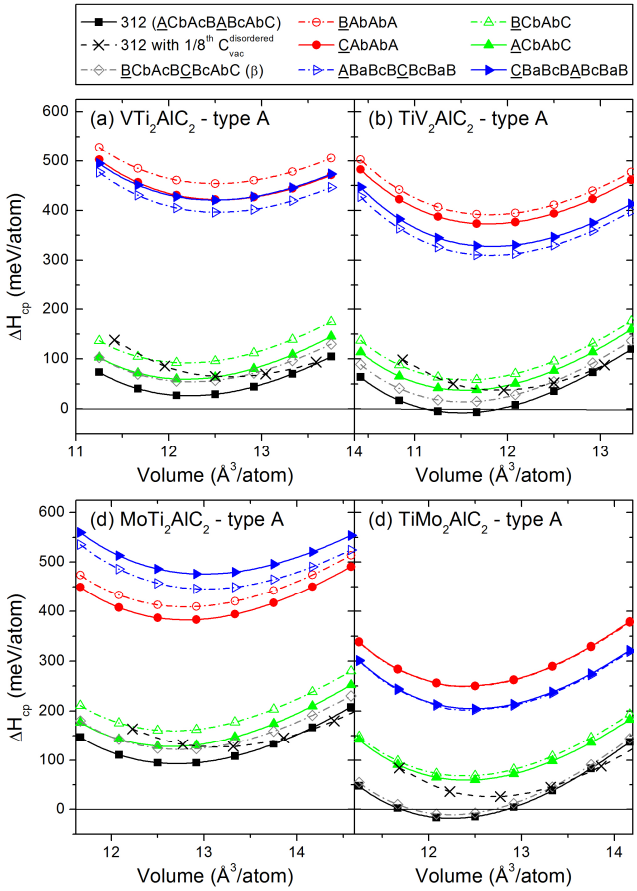

Fig. S6 Formation enthalpy ΔH_{cp} for different atomic stacking sequences of ordered (a) VTi2AlC2, (b) TiV2AlC2, (c) MoTi2AlC2, and (d) TiMo2AlC2, with type A layering. For the MAX phase stacking, disordered carbon vacancies have also been considered (×).

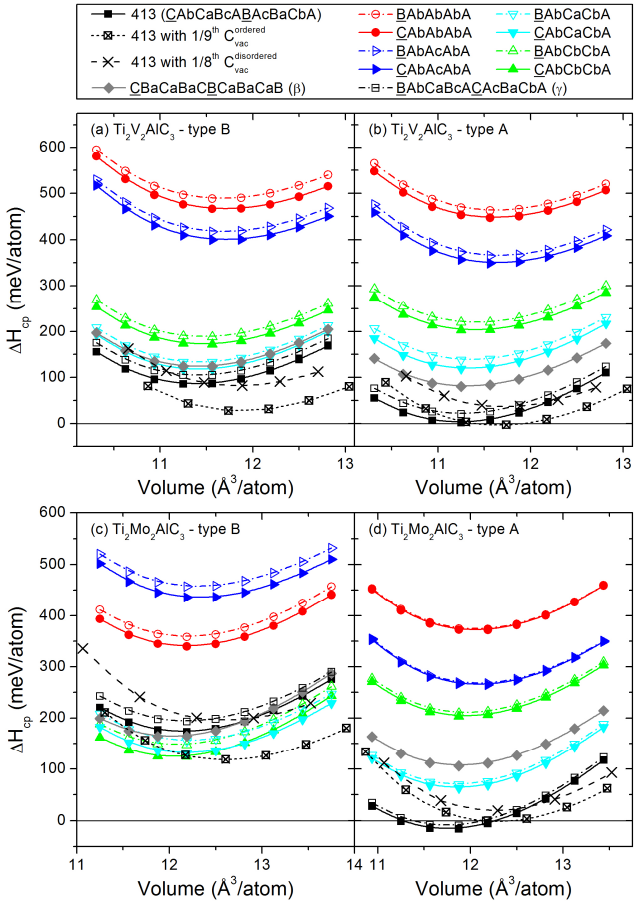

Fig. S7 Formation enthalpy ΔH_{cp} for different atomic stacking sequences of ordered $Ti_2V_2AlC_3$ of (a) type B and (b) type A, and $Ti_2Mo_2AlC_3$ of (c) type B and (d) type A. For the MAX phase stacking, disordered (×) and ordered (□) carbon vacancies have also been considered